Momentum-Transfer-Resolved Electron Energy Loss Spectroscopy of $BaBiO_3$: Anisotropic Dispersion of Threshold Excitation and Optically Forbidden Transition

Y. Y. Wang and V. P. Dravid

Department of Materials Science and Engineering, and Science and Technology Center for Superconductivity, Northwestern University, Evanston, Illinois 60208

N. Bulut,* P. D. Han, and M. V. Klein

Physics Department, and Science and Technology Center for Superconductivity, University of Illinois, Urbana, Illinois 61801

S. E. Schnatterly

Physics Department, University of Virginia, Charlottesville, Virginia 45221

F. C. Zhang

Physics Department, University of Cincinnati, Cincinnati, Ohio 45221

(Received 31 October 1994; revised manuscript received 10 April 1995)

Momentum-transfer-resolved electron energy loss spectroscopy of the valence band transitions in $BaBiO_3$ has revealed for the first time that dispersion of the excitation at the optical gap (~2 eV) and an optically forbidden transition at 4.5 eV are all anisotropic along [100] and [110]. The anisotropic dispersion of the threshold excitation cannot be described by a simple charge density wave picture but can be explained by a small exciton model proposed in this paper. The optically forbidden transition is found to agree well with a proposed molecular orbital model, where the transition is assigned as the excitation from the $O\ 2p\sigma$ nonbonding states to the empty Bi $6s$ state.

PACS numbers: 71.25.Jd, 78.20.–e

The electronic structure of oxide superconductors has been under intense scrutiny in recent years in hope of revealing clues about the mechanism of high-T_c superconductivity through the understanding of their normal state electronic structure. Equally important is the electronic structure of the parent insulating compounds. One such intriguing insulating compound is $BaBiO_3$.

$BaBiO_3$ has a monoclinic structure with two slightly different Bi-O bond lengths [1,2] and is the parent compound of $Ba_{1-x}K_xBiO_3$ and $Ba_{1-x}Pb_xBiO_3$ oxide superconductors. Similar to the undoped cuprates, $BaBiO_3$, with an odd number of electrons in the valence band, is an insulator despite the metallic prediction of the band structure calculations [3]. Owing to the different Bi-O bond lengths, a model involving charge density wave (CDW) instability was proposed to explain the insulating nature of $BaBiO_3$ [4]. The optical spectroscopy investigations have assigned the observed excitation near 2 eV as a transition across the CDW gap [5–7]. In photoemission experiments have, however, the charge disproportion is found to be small [8].

We have employed momentum-transfer- ($\boldsymbol{q}$-) resolved electron energy loss spectroscopy (EELS) to probe the momentum dispersion of the valence band excitations in $BaBiO_3$. For the first time, we report an optically forbidden transition (at ~4 eV) and effective mass of the optical gap (~2 eV), both of which have anisotropic property. In this paper, a molecular orbital model is proposed to interpret the forbidden transition and a good agreement is found between the experimental results and theoretical calculation. In addition, we also found that the anisotropic properties of the dispersion of the threshold excitation do not agree with a simple CDW picture but agree well with a small exciton model proposed here.

Inelastic electron scattering with $\boldsymbol{q}$ control has been effectively utilized to obtain information about the symmetry of electronic states and their dispersion in many solids [9–11]. Specifically, low loss EELS can reveal dynamic information about excitations, such as its effective mass through the relation

$$E(q) = E_0 + \frac{\hbar^2}{2m^*} q^2,$$

where E is the center of the excitation energy, q is the momentum transfer, and m^* is the effective mass. In addition, the presence of optically forbidden transitions can also be identified at higher q values. According to the Born approximation, the differential cross section of inelastic scattering can be written as

$$\frac{d^2\sigma}{dEd\Omega} \sim q^{-4} \sum_f |\langle \Psi_f | \exp(i\boldsymbol{q} \cdot \boldsymbol{r}) | \Psi_0 \rangle|^2 \times \delta(E_f - E_0 - E),$$

where Ψ_0 and Ψ_f are the initial-and final-state wave functions with energies as E_0 and E_f, respectively, and q is the momentum transfer. If r_c is the effective radius of the excitation, for $q < 1/r_c$, one can write

$$\exp(i\boldsymbol{q} \cdot \boldsymbol{r}) \cong 1 + (i\boldsymbol{q} \cdot \boldsymbol{r}) + (i\boldsymbol{q} \cdot \boldsymbol{r})^2/2 + \cdots.$$

For small q, the second term dominates the integral, permitting dipole-allowed transitions. For large q, the third

 0031-9007/95/75(13)/2546(4)$06.00

term, which contains monopole or quadrupole transitions, increases in strength relative to the dipole transitions [12].

Transmission electron microscopy (TEM) specimens of $BaBiO_3$ were prepared by mechanically polishing and subsequently ion beam thinning to electron transparency at liquid nitrogen temperature [13]. Energy loss spectra were obtained using a cold field emission TEM (Hitachi HF-2000) equipped with a Gatan 666 parallel detection electron energy loss spectrometer (PEELS). The peak width of the unscattered beam is ~0.5 eV. The zero loss peak is removed by fitting it with an asymmetric Lorentzian function [14]. The error of the peak center (or highest point) is estimated as $\Delta E/\sqrt{N}$ under the condition of $\Delta E \gg \delta E$, where ΔE is the width of the peak, δE is the energy step of the measurement, and N is the total number of count contained in the peak [14,15].

Figures 1(a) and 1(b) show the loss functions (after removal of zero loss function) at different $\boldsymbol{q}$ for $BaBiO_3$ along [100] and [110], respectively [16]. As $\boldsymbol{q}$ approaches zero, a pronounced excitation at 2.5 eV is seen in both spectra, which corresponds to the 2 eV excitation observed in optical spectroscopy [5–7,13]. With increasing q, the energy position of the 2.5 eV excitation along the [100] direction remains almost stationary, whereas the energy position of the same excitation along the [110] direction disperses towards higher energy. The dispersion with q of the excitation along [100] and [110] directions are shown in Fig. 2(a) [17].

In addition to the threshold excitation, another broad excitation appears at ~4.5 eV with increasing q, as can be seen in Fig. 1. The oscillator strength of this feature is stronger along [100] than along [110]. A Kramers-Kronig (KK) analysis of the loss functions indicates that the 4.5 eV excitation shifts down to 4.2 eV in ε_2 (imaginary part of the dielectric function), while the excitation at 2.5 eV in the loss function shifts to 2.1 eV in ε_2. By fitting the energy loss spectra with a combination of a Gaussian peak and a smooth background in the 4.5 eV energy region, the oscillator strengths of the forbidden transition for different momentum transfers are obtained and plotted against q^2 in Fig. 2(b), for both [100] and [110] directions. The linear relationship between the oscillator strength and q^2 is consistent with the major characteristic of either a monopole or a quadrupole transition. This dipole-forbidden transition is strongly anisotropic, as shown in Fig. 1. The ratio of the oscillator strength along [100] and [110] is estimated from the slopes of q^2 plots in Fig. 2(b) and is ~3.1 [18]. This excitation is assigned to be a transition from the nonbonding oxygen $2p\sigma$ orbital of the valence band to the empty Bi $6s$ state.

Our choice for the nonbonding O($2p$) states is the energy level which is ~2 eV below the Fermi level in accord with the band structure calculations [3]. This is roughly consistent with the peak position of the dipole-forbidden transition (which occurs at ~4.2 eV), ~2 eV above the threshold of the dipole-allowed transition.

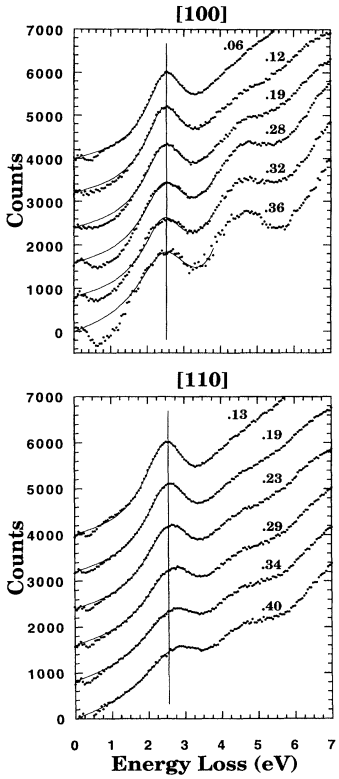

FIG. 1. Energy loss spectra for $BaBiO_3$ with different momentum transfer $\boldsymbol{q}$ in [100] and [110] directions. The unit of the insert number is $Å^{-1}$.

Since the O($2p$) nonbonding states do not disperse [3], we can use a molecular orbital model to construct the symmetry of the transitions associated with O($2p$) nonbonding states [19]. We consider the linear combinations of the six O($2p\sigma$) atomic orbitals with e_g symmetry around the Bi ion in $BaBiO_3$. The two nonbonding states can be written as

$$\phi_1 = \tfrac{1}{2}(p_x - p_y - p_{-x} + p_{-y}),$$

$$\phi_2 = \frac{1}{\sqrt{12}}(p_x + p_y - 2p_z - p_{-x} - p_{-y} + 2p_{-z}),$$

where p_i ($i = \pm x, y$, or z) is the O($2p\sigma$) wave function at the i atom position. ϕ_1 has a $d(x^2 - y^2)$ symmetry as illustrated in Fig. 3, and ϕ_2 has a $d(3z^2 - r^2)$ symmetry. Because of the symmetry, these wave functions are orthogonal to the Bi $6s$ state, and the dipole transitions from these states to Bi $6s$ are optically forbidden. Since the forbidden transition is between s-like and d-like states, it is referred as a quadrupole transition. Furthermore, the amplitude of ϕ_1 is large along [100] and zero along [110]. This leads to a strong anisotropy of the strength for the quadrupole transition. To calculate quantitatively, we denote $\langle \phi_s | x^2 | p_x \rangle = \alpha$ and $\langle \phi_s | y^2 | p_x \rangle = \beta$, with ϕ_s as the Bi $6s$ wave function, and $|\alpha| > |\beta|$. We obtain the transition matrix

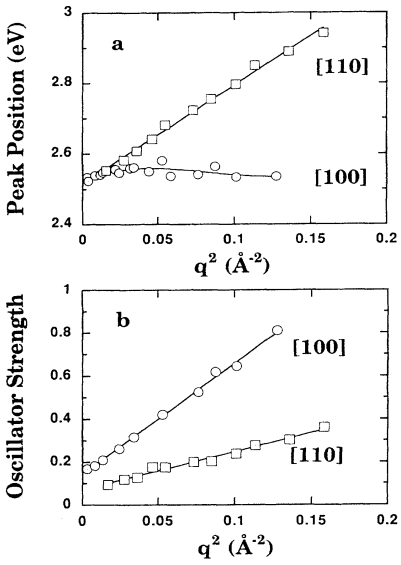

FIG. 2. (a) The peak position of 2.5 eV vs q^2 along [100] and [110]. (b) The oscillator strength of 4.5 eV excitation vs q^2 along [100] and [110].

elements along [100] as $|\langle\phi_s|x^2|\phi_1\rangle|^2 = (\alpha - \beta)^2$ and $|\langle\phi_s|x^2|\phi_2\rangle|^2 = \frac{1}{3}(\alpha - \beta)^2$. The transition matrix elements along [110] are $|\langle\phi_s|(x + y)^2/2|\phi_1\rangle|^2 = 0$ and $|\langle\phi_s|(x + y)^2/2|\phi_2\rangle|^2 = \frac{1}{3}(\alpha - \beta)^2$. The ratio of the transition strength between [100] and [110] is 4, which compares favorable with the experimental result of ~3.1. This model also predicts the ratio of the strength for the forbidden transition between [100] and [111] to be (31)(4)/ ~ 8, consistent with our experimental observations that the oscillator strength in [111] is significantly weaker than the one in [110].

The effect of the nonbonding O $2p\pi$ orbital on the optically forbidden transition is much smaller due to a smaller wave-function overlap between O $2p\pi$ and Bi $6s$ states. From six O $2p\pi$ atomic states (two for each O atom) with one Bi ion, we can construct three d-wave molecular orbitals (d_{xy}, d_{yz}, d_{xz}), and three p-wave molecular orbitals (along x, y, and z directions). The p-wave orbitals are dipole-allowed transitions to the Bi($6s$) state, but the strength is much weaker due to the small wave-function overlap. This is consistent with the optical measurements [7,20].

We now discuss the dispersion of the optical gap in the electron energy loss spectra. As shown in Fig. 2(a), the peak position is essentially dispersionless along [100], while it is proportional to q^2 along [110] [21]. In 1977, Fields, Gibbons, and Schnotterly reported anisotropic dispersion of an exciton in LiF along [100] and [110] [22]. However, comparing with the exciton in LiF, the anisotropy in $BaBiO_3$ is unusually large at a small momentum transfer. It will be shown that this unusual dispersion disagrees with a simple CDW model but agrees well with a small exciton model.

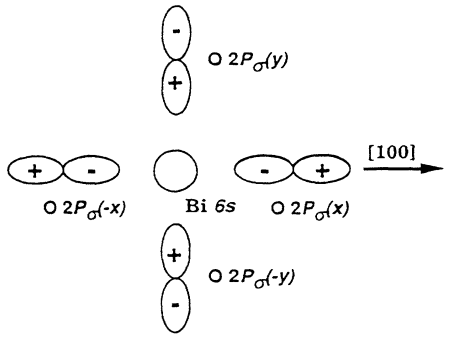

FIG. 3. Illustration of the nonbonding wave function ϕ_1, which has $d(x^2\text{-}y^2)$ symmetry. The amplitude of this wave function is zero along the [110] direction, which results in the weaker forbidden transition [110].

First, we examined the dispersion in CDW model. In this model, a periodic variation in bond length—which doubles the unit cell and results in an insulator state—opens a band gap [4]. The CDW quasiparticle dispersion relation is $E^{\pm}(\boldsymbol{p}) = \pm\sqrt{\varepsilon_p^2 + \Delta^2}$ measured respective to the chemical potential, where Δ is the CDW gap, and

$$\varepsilon\boldsymbol{p} = -2[\cos(p_x) + \cos(p_y) + \cos(p_z)].$$

Based on this formula, for the perfect nesting, the numerical calculation of the dielectric function $\varepsilon_2(\boldsymbol{q}, \omega)$ indicates that the energy band gap is isotropic and dispersionless in terms of momentum transfer $\boldsymbol{q}$. This calculated result agrees with the dispersion result along [100] but disagrees with the result along [110]. If the Fermi surface is away from the perfect nesting, the calculation indicates that the band gap is isotropically dispersive as q^2, which also disagrees with the anisotropic nature observed in the present experiment. Therefore, it is very unlikely that the band picture can explain such strong anisotropy, where the dispersion may be expressed as $\omega(\boldsymbol{q}) \sim \omega(0) + C\sin(q_x)\sin(q_y)$. Next, we will propose a small exciton model to describe the strong anisotropic dispersion.

We use Rice and Sneddon's local description picture [23] and consider a small exciton where the quasiparticle and quasihole are bound to the nearest neighbor in the Bi cubic lattice due to the Coulombic interaction. Furthermore, the quasiparticle sits on sublattice A only, and the quasihole sits on sublattice B only. Shown in Fig. 4 are the two optically active (with an odd parity) local excitons in the x-y plane with two wave functions for quasihole as

$$\boldsymbol{P}_1^{\text{hole}} = \tfrac{1}{2}(\varphi_x - \varphi_{-x} + \varphi_y - \varphi_{-y}),$$

$$\boldsymbol{P}_2^{\text{hole}} = \tfrac{1}{2}(\varphi_x - \varphi_{-x} - \varphi_y + \varphi_{-y}),$$

where φ_i ($i = \pm x, y$, or z) is the wave function at the site i. Because of the effective hopping integral t' of the quasiparticle, the excitons can move between the next nearest neighbor sites which belong to the same sublattice.

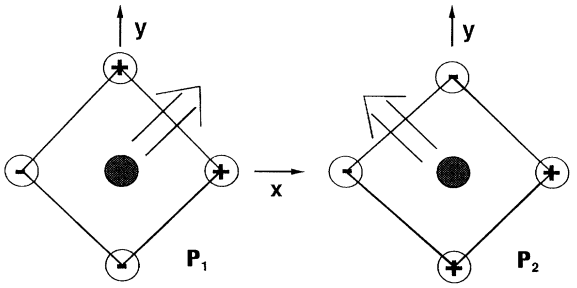

FIG. 4. Two small excitons in the x-y plane with a p symmetry. The exciton consists of a quasiparticle (solid circle) at sublattice A and a linear combination of four nearest neighbor quasiholes (hollow circle) state at sublattice B. The signs indicate the relative phases of quasihole. The arrows indicate the directions of the exciton motion with the strongest oscillator strength.

Neglecting the kinetic energy, the optical active gap is given by the energy of the local excitons in Fig. 4. By including the effective hopping of the quasiparticle and letting ϑ be the angle between $\boldsymbol{q}$ and the x axis, the excitons dispersion induced by t' can be calculated for small $\boldsymbol{q}$ as [24]

$$2t' \sin(q_x)\sin(q_y) \approx t'q^2 \sin(2\vartheta) \quad \text{for } \boldsymbol{P}_1 ,$$

$$-2t' \sin(q_x)\sin(q_y) \approx -t'q^2 \sin(2\vartheta) \quad \text{for } \boldsymbol{P}_2 .$$

The oscillator strength of the optical transition is proportional to $|I_n|^2$, where $I_n = \langle \mathrm{GS}|\hat{\boldsymbol{q}} \cdot \boldsymbol{r}|P_n\rangle$, with $|\mathrm{GS}\rangle$ as the ground state, $\hat{\boldsymbol{q}}$ as the unit vector of $\boldsymbol{q}$, and $n = 1, 2$ representing the two excitons. By invoking the symmetry, we found that $|I_1|^2 = C[1 + \sin(2\theta)]$ and $|I_2|^2 = C[1 - \sin(2\theta)]$ with C as a constant. The dispersion in this model shows a strong anisotropy: dispersionless along [100] and dispersive along [110]. The oscillator strength of the model shows that along [110] only the exciton P_1 is optically active, while along $[1\bar{1}0]$ only the exciton P_2 is optically active. The exciton energy with a stronger oscillator strength always shifts towards higher energy. All these are qualitatively consistent with our experimental results.

In summary, we have performed $\boldsymbol{q}$-resolved EELS measurements on the insulating compound $BaBiO_3$. The data have two important features: an anisotropic optically forbidden transition at 4.5 eV and the anisotropic dispersion of the threshold excitation at 2.5 eV. For the forbidden transition, we have proposed a molecular orbital model and assigned the transition as a quadrupole transition from d-like molecular orbital of nonbonding O $2p\sigma$ states to the Bi $6s$ state. For the anisotropic dispersion of the threshold excitation at 2.5 eV, numerical calculations indicate that a simple tight binding CDW approximation does not account for this anisotropy. However, we found that the anisotropic properties can be derived from a small exciton proposed in the paper.

We would like to thank S. L. Cooper, J. P. Zhang, and T. M. Rice for stimulating discussions. The research is supported by the National Science Foundation with Grant No. NSF-DMR-91-20000 and Contract No. DMR 91-20055.

*Present address: Department of Physics, University of California, Santa Barbara, California 93106

[1] D. E. Cox and A. W. Sleight, Solid State Commun. **19**, 969 (1976).
[2] L. F. Schneemeyer *et al.*, Nature (London) **335**, 421 (1988).
[3] L. F. Mattheiss and D. R. Hamann, Phys. Rev. Lett. **60**, 2681 (1988).
[4] M. J. Rice and Y. R. Wang, Physica (Amsterdam) **157C**, 192 (1989).
[5] H. Sato *et al.*, Nature (London) **338**, 241 (1989).
[6] S. H. Blanton *et al.*, Phys. Rev. B **47**, 996 (1993).
[7] M. A. Karlow *et al.*, Phys. Rev. B **48**, 6499 (1993).
[8] Z. X. Shen *et al.*, Phys. Rev. B **40**, 6912 (1989).
[9] H. Reather, *Excitation of Plasmon and Interband Transitions by Electrons,* Springer Tracts in Modern Physics (Springer-Verlag, Berlin, 1980), Vol. 88.
[10] S. E. Schnatterly, in *Solid State Physics* (Academic Press, New York, 1979), Vol. 14, pp. 275–358.
[11] N. Nucker *et al.*, Phys. Rev. B **44**, 7155 (1991).
[12] J. J. Ritsko *et al.*, Phys. Rev. Lett. **36**, 210 (1976).
[13] Y. Y. Wang *et al.*, Phys. Rev. B **47**, 14 503 (1993).
[14] Y. Y. Wang *et al.*, Ultramicroscopy (to be published).
[15] G. Gilbert and J. W. Addington, Gen. Phys. D **5**, 1780 (1972).
[16] The axis index is based on a pseudocubic structure of the material.
[17] By fitting the 2.5 eV excitation with a Gaussian function and a rising background function, we find that the peak position of the Gaussian function is flat along [100] but dispersive along [110] with a different slope value.
[18] The background of the data fitting for the forbidden transition is kept consistent throughout. The uncertainty of the ratio is estimated to be about ± 1 with a reasonable background variation.
[19] W. A. Harrison, *Electronic Structure and the Properties of Solids* (Dover Publication, New York, 1989).
[20] Y. Y. Wang *et al.*, Phys. Rev. B **48**, 16 006 (1993).
[21] The influence of the energy position of the 2 eV excitation by the forbidden transition is very small according to our calculation.
[22] J. R. Fields, P. C. Gibbons, and S. E. Schnatterly, Phys. Rev. Lett. **38**, 430 (1977).
[23] T. M. Rice and L. Sneddon, Phys. Rev. Lett. **47**, 689 (1981).
[24] In deriving these dispersions, the phases of the quasihole wave functions, indicated by the signs in Fig. 4, are important. Because of these phases, the effective hopping integrals of the exciton along [110] and $[1\bar{1}0]$ have opposite signs. For P_1 exciton, for example, it is $-t'/2$ along [110] and $+t'/2$ along $[1\bar{1}0]$. The dispersion is, therefore, $-t'\cos(q_x + q_y) + t'\cos(q_x - q_y)$, which leads to a product of two sine functions given in the text. A similar anisotropic result has been obtained with more detailed 3D calculations.